Desalination and Water Treatment
www.deswater.com

doi: 10.5004/dwt.2019.24764

171 (2019) 144–157
December

Application of composite adsorbents prepared from waste PS and PET for removal of Cr and Cu ions from wastewater

Muhammad Ilyas[a,*], Waqas Ahmad[b], Hizbullah Khan[a], Imtiaz Ahmad[b]

[a]*Department of Environmental Sciences, University of Peshawar, Peshawar, Khyber Pakhtunkhwa, Pakistan, Tel. +923078064028; emails: sirfilyas@yahoo.com (M. Ilyas), hizbullah@uop.edu.pk (H. Khan)*
[b]*Institute of Chemical Sciences, University of Peshawar, Peshawar, Khyber Pakhtunkhwa, Pakistan, emails: waqasahmad@uop.edu.pk (W. Ahmad), Patwar2001@yahoo.co.in (I. Ahmad)*

Received 20 April 2019; Accepted 28 July 2019

ABSTRACT

In this study, waste polystyrene and polyethylene terephthalate were used to prepare efficient adsorbents by incorporating with bentonite clay and biochar, for removal of Cr and Cu ions from wastewater. In waste polymers as matrix, biochar and bentonite clay were incorporated as fillers in different compositional ratios to prepare biochar/bentonite/waste polystyrene (wPS/C/Bt) and biochar/bentonite/waste polyethylene terephthalate (wPET/C/Bt) composites. The composites were characterized by SEM, specific surface area analysis and FTIR analysis. The optimum conditions for maximum adsorption of Cr^{6+} and Cu^{2+} ions from aqueous solution on the wPS/C/Bt and wPET/C/Bt composites were found to be: pH 3 for Cr^{6+} and pH 6 for Cu^{2+}, contact time of 90 min, temperature 60°C, adsorbent dose of 0.20 g and Cr^{6+} and Cu^{2+} ions concentration of 30 mg/L. The concentration of Cr^{6+} and Cu^{2+} ions was determined by atomic absorption spectrophotometer and the adsorption efficiencies of the composites were calculated under optimal condition. Results shown that maximum removal of Cr^{6+} and Cu^{2+} ions from aqueous medium attained over wPS/C/Bt adsorbent was 77.56% and 79.80%, respectively, while that of wPET/C/Bt adsorbent was 90.10% and 86.30%, respectively. Adsorption kinetics was studied using different kinetics models, the results were also evaluated by applying various adsorption isotherm models. Kinetic study shows that the adsorption of Cr and Cu ions follows pseudo-second-order kinetics. The experimental data best fitted to both the Langmuir and Freundlich isotherm model. The values of thermodynamic parameters such as entropy ($\Delta S°$), Gibbs free energy ($\Delta G°$) and enthalpy ($\Delta H°$) show that the adsorption process is feasible, spontaneous and endothermic in nature. This investigation demonstrated that the novel composite wPET/C/Bt has a large potential for the removal of Cr^{6+} and Cu^{2+} ions from industrial wastewater.

Keywords: Biochar-bentonite; Polymers; Composite; Metal adsorption; Kinetics and isotherm

1. Introduction

Management of municipal and industrial wastewater has become an inevitable challenge of the modern day world [1,2], because of the extensive industrialization and rapid growth in human population around the world [3,4]. Excessive urbanization is associated with huge consumption of industrially manufactured goods containing various levels of trace and heavy metals, which are ultimately disposed of to the environment as waste, causing severe environmental pollution [5]. Various types of heavy metals find their way to water bodies and enter into food chain and poses serious health risks to humans. Different heavy metals have been reported to cause different physiological toxicities, but in general, trace and heavy metals are known to be associated with damage of bones, liver, kidney, nerves and also block the enzyme functional groups [6].

---

[*] Corresponding author.

1944-3994/1944-3986

Among various heavy metals, chromium (Cr^{6+}) and copper (Cu^{2+}) are of great concerns, since these are widely used in industries, as a result of these, high concentrations of these metals are found in industrial and municipal sewages. Cr compounds are principally used as wood preservative in wood processing industries, in pigments in textile industry, in leather tanning and finishing and in electroplating industry for corrosion resistance. Wastewater contains Cr in both hexavalent and trivalent forms, having oxidation states +6 and +3, respectively. It is reported that Cr is mutagenic in +6 form and bio element in +3 states [7]. Studies reveal that Cr^{6+} is readily absorbed by the cell as compared with Cr^{3+}. Inhalation, dermal contact, and ingestion are the common routes through which Cr enters into the human body. The essential wellbeing dangers caused by Cr are developmental and reproductive problems, skin allergies, nasal and lung ulcers and cancers, and may also cause death in excess uptake [8]. The US Environmental Protection Agency (USEPA) recommended 100 $\mu g\ L^{-1}$ concentration of Cr in drinking water [7]. In several instances, natural Cr (+6) may surpass drinking water treatment measures. For example, a portion of the recorded qualities in groundwater located near ultramafic rocks enormously surpass the drinking water limits (50 $\mu g\ L^{-1}$) of World Health Organization (WHO). These areas incorporate the province of New Caledonia; the Mojave Desert, United States; and La Spezia, Italy; at 700, 60, 5–73 $\mu g\ L^{-1}$, respectively [9,10].

Likewise, copper (Cu) is utilized in numerous industrial applications, for example, etching, electroplating, and metal finishing [11], wood preservation, petroleum refining, pulp, paper industries, etc. [12], which releases Cu directly to the environment. Besides, other sources which contain Cu, include animal wastes, fungicidal sprays and fertilizers [13], some foods particularly mushrooms, liver, shell fish, chocolates and nuts, packaging containers used for water, drink and food, leads to release of Cu to the environment. Cu has been accounted to cause Wilson's disease (neurotoxicity) and kidney failure [14]. In some cases, Cu is known to cause enlarged liver and jaundice [15]. Additionally, Cu^{2+} at low concentration is considered as an exceptionally poisonous metal [16]. According to USEPA, in industrial effluents the allowable limit of Cu^{2+} ion was set to be 1.3 mg L^{-1} [17]. Therefore, $Cr^{6+}$and copper Cu^{2+} removal from wastewater is fundamental in view of their incessant occurrence in wastewater [18].

Over the time various techniques are developed to cater for the removal of heavy metals from wastewater, which include membrane separation, flocculation or coagulation, electrochemical treatment, chemical reduction/oxidation, complexation, solid-phase adsorption, chemical precipitation, filtrations, bio-sorption photocatalytic reduction, adsorption, electrochemical precipitation, membrane separations, chemical precipitation, ion exchange and reduction [19–27]. Each of these innovations has its own particular impediments, for example, toxic sludge (solid residue) generation, intermediate poisonous chemical production, higher cost because of the high energy requirement, incomplete removal and time consuming [28]. However, among these the adsorption process seems to hold promise in removal of heavy metals including Cu and Cr ions. Various solid adsorbents used for this purpose include kaolin [29], natural zeolites [30], peat [31], coal [32] and activated carbon [33]. Other researchers have examined the adsorption of Cr and Cu ions from aqueous solutions on polyaniline/palygorskite composite, polyaniline, expanded perlite, acid activated palygorskite, crosslink cationic starch and palygorskite [18,34–38].

Management of solid-plastic waste is another environmental issue, since plastics are produced and consumed on large scale, whereas environment being the sole sink of these waste. The expanding utilization of plastics has resulted in the landfill depletion [39]. Currently, the rivers, seas and oceans act as a sink for other plastic debris as well as polystyrene and polyethylene terephthalate [40]. Various techniques used for handling the waste plastics have been suggested which include land filling, incineration, recycling, conversion into gaseous and liquid fuels [41]. A more suitable option can be its utilization as adsorbent for treatments of polluted water in composite form.

In the current study, waste polystyrene and polyethylene terephthalate are converted into the solid composite adsorbents by incorporation with char and bentonite clay and are used for removal of Cr^{6+} and Cu^{2+} ions from wastewater. This study is aimed at: (i) removal of the toxic Cr^{6+} and Cu^{2+} ion from wastewater and (ii) reducing the environmental pollution associated with solid wastes and plastic debris lying around the streets, roads and drains.

2. Experimental

2.1. Sample collection and preparation

Biochar, prepared from wood was provided by the University of Agriculture (Peshawar, Pakistan). Bentonite clay was purchased from Karachi market Khyber Bazaar Peshawar, Pakistan. Both biochar and bentonite clay were ground and screened through a sieve, with pore size 250 μm. Samples of waste polystyrene or styrofoam (wPS) and waste polyethylene terephthalate (wPET) were collected from the municipal solid wastes. The wPS and wPET were washed with distilled water, dried at room temperature and then shredded into small flakes.

The metals stock solution containing 1,000 mg L^{-1} of Cr^{6+} and Cu^{2+} ions was prepared by dissolving potassium dichromate ($K_2Cr_2O_7$) and copper(II) sulfate ($CuSO_4$), in 1 L of deionized water.

2.2. Preparation and characterization of the composite adsorbent

The composite adsorbents were prepared by incorporating biochar and bentonite clay as filler in wPS and wPET matrix in different ratios by mass. In typical procedure, wPS or wPET were dissolved in toluene separately, and stoichiometric amounts of biochar and bentonite clay were dispersed in each by sonication at 35°C for 1 h. The suspension was poured into Petri dish and dried overnight. The composite prepared from waste polystyrene-biochar and bentonite clay was coded as wPS/C/Bt and that of waste polyethylene terephthalate was coded as wPET/C/Bt. Different composite samples were prepared with different percentage by mass of fillers, that is, biochar and bentonite in polymer matrix.

The composite samples were characterized by SEM (JSM-5910, JEOL, Japan), FTIR (Spectrum Two, S.No: 103385) analysis and specific surface area analysis (SAA; NOVA2200e, Quantachrome, USA).

2.3. Adsorption experiments

Adsorption of Cr and Cu ions on the composite adsorbents was studied in batch mode experiments. About 50 mL of stock solution containing 1,000 mg L^{-1} of Cr^{6+} and Cu^{2+} was taken in Erlenmeyer flask and about 0.5 g of adsorbent was added and stirred using magnetic stirrer. The adsorbent was recovered by filtration and the filtrate was subjected to analysis. The adsorption experiments were carried out under different conditions of contact time (15, 30, 45, 60, 90 min), adsorbent amount (0.05, 0.10, 0.15, 0.20 g), pH (1–7), and temperature (30°C, 40°C, 50°C, 60°C) to optimize the adsorption parameters [12].

2.4. Analyses and calculations

The concentration of Cr and Cu ions in the filtrate was analyzed by atomic absorption spectrophotometer (AAnalyst 700, PerkinElmer, USA) equipped with air flame mode using conditions as per Table 1.

From the concentration of metal ion in filtrate sample, the % removal was calculated as;

$$\%\text{MR} = \frac{[(C_0 - C_i)\times 100]}{C_0} \tag{1}$$

where C_i and C_0 represent the final and initial concentration (mg L^{-1}). The amount of equilibrium adsorption, q_e (mg g^{-1}), was calculated using the following relation [42].

$$q_e = \frac{[(C_0 - C_i)\times v]}{m} \tag{2}$$

where v is the volume (L) of stock solution and m is the adsorbent weight (g). For all tests carried out, the mean values only of triplicate were presented.

Adsorption kinetics was investigated by applying different rate equations. Construction of linear plots was studied by applying pseudo-first-order and pseudo-second-order kinetic model. The pseudo-first-order rate constant was calculated using following Eq. (3) [43]:

$$\ln(q_e - q_t) = \ln q_e + k_{1t} \tag{3}$$

Table 1
Atomic absorption spectrophotometer specifications for Cr^{6+} and Cu^{2+}

Parameters	Cr^{6+}	Cu^{2+}
Wavelength (nm)	357.9	324.8
Fuel gas	Air acetylene	Air acetylene
Air flow (L/min)	17	17
Lamp current (mA)	25	15
Energy	75	68
Slit width	0.7	0.7

The pseudo-second-order rate constant was determined using following equation [44]:

$$\frac{t}{q_t} = \frac{t}{q_e} + \frac{1}{K_2 q_e^2} \tag{4}$$

Different adsorption isotherms were also applied to investigate the nature of adsorption. The Langmuir isotherm equation was used in the following form [45];

$$\frac{C_e}{q_e} = \frac{1}{KQ_{\max}} + \frac{C_e}{Q_{\max}} \tag{5}$$

The Freundlich adsorption isotherm was applied as following equation [46];

$$\ln q_e = \ln K_f + \frac{1}{n}\ln C_e \tag{6}$$

where q_e represent the concentration adsorbed on the composite (mg g^{-1}), C_e is the equilibrium concentration of the metal ion (mg L^{-1}), while the constant and the adsorption coefficient is represented by n and K_f for the model, respectively.

3. Results and discussion

Preliminary adsorption experiments were carried out for 1 h contact time, 60°C temperature and adsorbent to solution ratio of 0.10 g/20 mL, the % adsorption of Cr and Cu ion is given in Fig. 1. The waste polymers were mixed with the biochar and bentonite clay in different compositional ratios. The efficient adsorbent of utilizing waste polymer of 10% and biochar and bentonite clay of 20, 20% were selected for further experiments. Results indicates that the composites samples, that is, wPS/C/Bt:1:2:2 and wPET/C/Bt:1:2:2 show greater tendency for the adsorption of Cr^{6+} and Cu^{2+} ions than that of the fillers. This difference of adsorption potential is due to

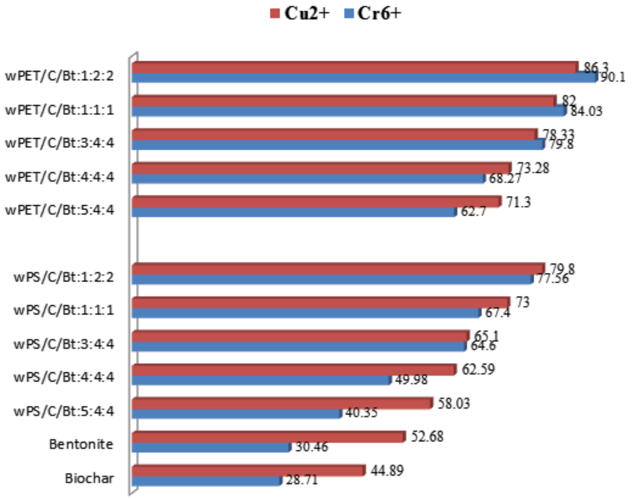

Fig. 1. % Adsorption efficiency of composite adsorbents prepared in the laboratory at various compositions.

diverse metal ions mechanism. In case of adsorption by only biochar and bentonite, the removal efficiency for both Cr^{6+} and Cu^{2+} ions is very low; whereas in case of the composite adsorbents, the adsorption efficiency of both ions is higher than the pure carbon and bentonite, which shows the clear advantage of the composite adsorbents. Among the composite adsorbents, wPS/C/Bt:1:2:2 and wPET/C/Bt:1:2:2 composites shown the highest removal efficiency for both ions, in case of Cr^{6+} the % removal was 77.56% and 90.10 %, while for Cu^{2+} the % removal was 79.80% and 86.30%, respectively. This difference in adsorption efficiency is due to diverse metal ions mechanism. When the fillers were utilized as an adsorbent, at the point only chelation existed between metal ions and fillers. However, three removal mechanisms, electrostatic attraction, ion exchange, and chelation mechanism existed simultaneously when the composite adsorbents was used [34]. As a result, the adsorption efficiency of the composite adsorbents was larger than that of fillers.

3.1. Characterization of composite adsorbents

The composite adsorbents prepared in the laboratory were characterized by SEM and FTIR analysis. The SEM micrographs of the biochar, bentonite clay, waste polystyrene (wPS) and waste polyethylene terephthalate (wPET), wPS/C/Bt:1:2:2 and wPET/C/Bt:1:2:2 are displayed in Figs. 2a–f. The SEM micrograph of biochar (Fig. 2a), shows non-uniform granular morphology. Fine grains and lumps are visible indication different sized of the biochar particles, which ranges in sizes from less than 5 micron to as large as 30 micron. The surface morphology of bentonite (Fig. 2b) depicts mesoporous structure, characteristics of aluminosilicates, with some extraneous particles spread on the surface. The micrograph of wPS displayed in Fig. 2c shows a spongy structure with wide pores openings, formed from interconnected polymer films. In Fig. 2d SEM images highlighting the porosity of wPET are shown. The surface features of wPET and region of both external and internal structure and in addition the unfilled spaces between the particles can be seen. The SEM images of the composite adsorbent wPS/C/Bt:1:2:2 are shown in Fig. 2e. Clearly, surface morphology shows the stuffing of biochar and bentonite inside the pores of wPS and finally resulted in uniform microcellular foaming in the composite. On the other hand, the wPET/C/Bt:1:2:2 SEM micrographs are shown in Fig. 2f. It shows that in the holes of wPET, the biochar and bentonite were embedded and combine tightly.

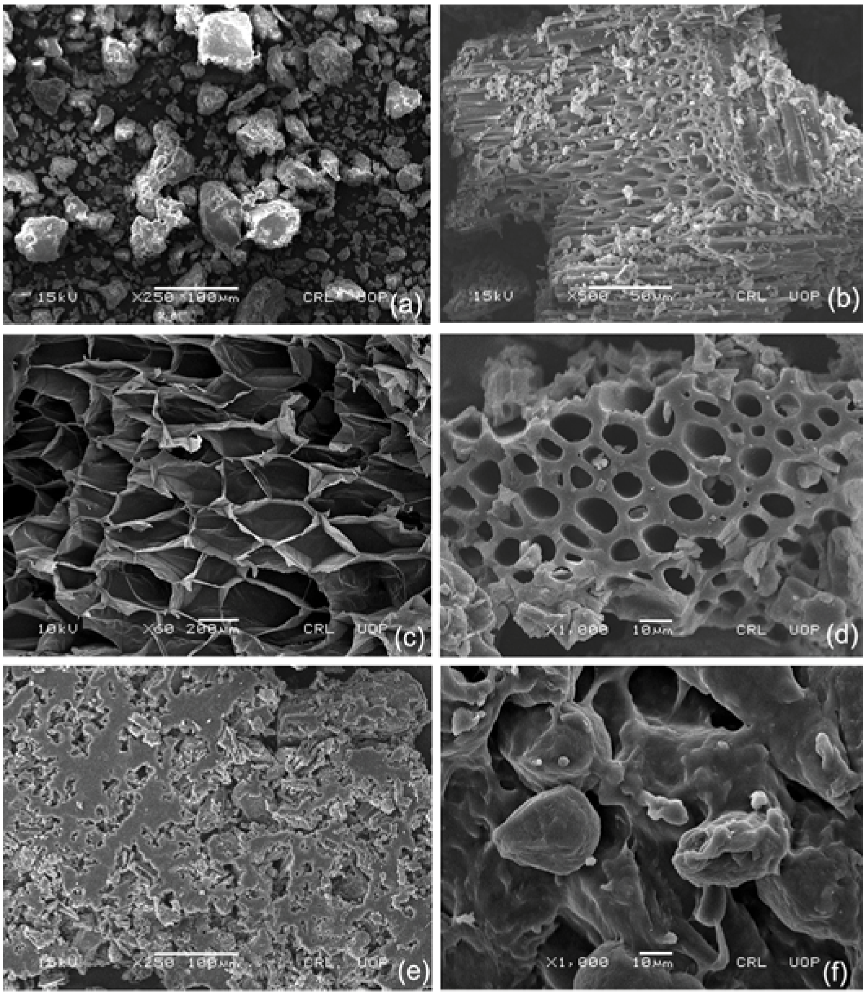

Fig. 2. SEM images of (a) biochar, (b) bentonite clay, (c) wPS, (d) wPET, (e) wPS/C/Bt:1:2:2 and (f) wPET/C/Bt:1:2:2.

In the surface cracks or pores of wPET, there were many club-shaped crystals, which had a much larger size having 9–10 and 5–6 μm length and diameter, respectively.

Figs. 3a–f shows FTIR spectra of the waste polymers, fillers and the composite adsorbents. The FTIR spectrum of the biochar sample shows a broad peak at around 1,620 cm^{-1} which corresponds to aromatic C=C bonds, a weak peak positioned at 1,012 cm^{-1} indicates C–O bonds for carbon oxygen linkage resulted due to surface oxidation [47,48]. The spectrum of bentonite clay shows a peak at 3,625 cm^{-1} which indicates O–H bond, due to surface moisture. Peaks positioned at 1,635 and 989 cm^{-1} which indicates H–O–H and Al–O bonds, which indicates the aluminate structure of the clay [49,50]. The FTIR spectrum of wPS shows peaks centered at around 3,000 and 2,800 cm^{-1} corresponding to aromatic C–H and methylene C–H bonds. Multiple peaks positioned at 1,630 and 1,500 cm^{-1} indicates aromatic C=C, a peak around 1,447 cm^{-1} indicate methylene C–H vibration. These configurations agree with the structure of polystyrene [51,52]. The characteristic infrared absorptions bands of wPET (Fig. 3d) at 1,697 cm^{-1} (C=O, stretch); 1,249 cm^{-1} (C=C, stretch); 1,092 cm^{-1} (C–O, stretching vibration); 1,010 cm^{-1} (C–O–C, stretching); 721 cm^{-1}(C–H, stretch); 521 cm^{-1} (C–H, stretch) are clearly observed [49,50]. The wPS/C/Bt:1:2:2 composite FTIR spectrum is shown in Fig. 3e. The absorption bands were detected at 3,630 cm^{-1} (O–H, stretch); 2,919 cm^{-1} (=CH_2, stretching); 1,599 cm^{-1} (C=C, stretching); 1,493 cm^{-1} (C=C, stretching); 1,451 cm^{-1} (CH_2 stretching); 1,013 cm^{-1} (C–O, stretching); 698 cm^{-1} (C–H, stretching) and 521 (C–H, stretching) cm^{-1} [49,51–53]. The FTIR spectrum of the wPET/C/Bt:1:2:2 (Fig. 3f) presented the absorption bands in the region at 3,630 cm^{-1} (O–H, bending vibration); 1,634 cm^{-1} (H–O–H, bond); 1,013 cm^{-1} (C–O, bending vibration); 698 cm^{-1} (C–H, bending vibration) and 521 cm^{-1} (C–H, bending vibration). The new wPS/C/Bt and wPET/C/Bt composite adsorbent had functional groups of both the fillers and waste polymers, and therefore its adsorption efficiency was considered to be better than that of fillers or waste polymers.

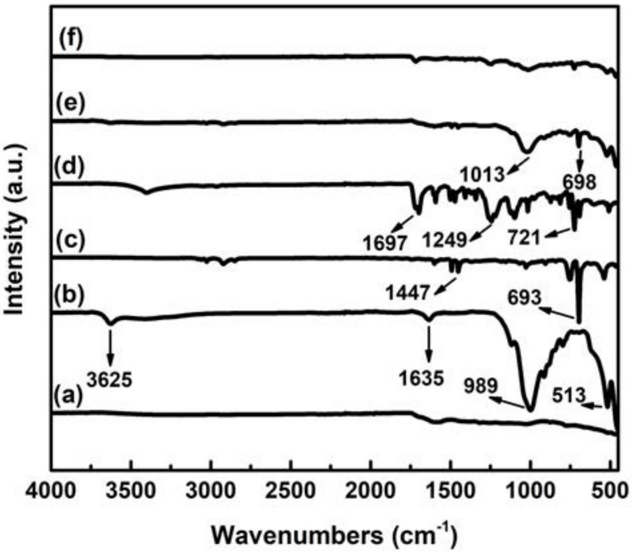

Fig. 3. FTIR spectra of (a) biochar, (b) bentonite, (c) wPS, (d) wPET, (e) wPS/C/Bt:1:2:2 and (f) wPET/C/Bt:1:2:2.

The surface properties, that is, BJH surface area (SBJH), BET surface area (S_{BET}), pore volume and pore radius of the fillers and composite adsorbents were determined using N_2 adsorption isotherms at 77.35 K. The results are given in Table 2. The results of surface analysis (Table 2) indicate that in case of biochar and bentonite the calculated S_{BJH} was found to be 14.10 and 22.37 $m^2 g^{-1}$, the S_{BET} was 18.37 and 43.27 $m^2 g^{-1}$, with pore radius of 14.90 Å and 16.62 Å and pore volume of 0.01 and 0.02 $cm^3 g^{-1}$, respectively. In case of wPS/C/Bt:1:2:2 and wPET/C/Bt:1:2:2 composite, the S_{BJH} was found to be 55.59 and 50.68 $m^2 g^{-1}$, the S_{BET} was found to be 44.95 and 58.53 $m^2 g^{-1}$, with pore radius of 27.71 Å and 27.68 Å having pore volume of 0.07 and 0.06 $cm^3 g^{-1}$, respectively. It is clear from the data that the composite adsorbents possess a high surface area and large pore dimensions than the fillers. Hence, the composite sample holds better adsorption potential compared with the fillers.

3.2. Investigation of the adsorption parameters

Initial adsorption experiments were carried out at constant conditions such as contact time (1 h), stirring speed (100 rpm), temperature (ambient) and adsorbent to solution ratio of 0.10 g/20 mL in order to screen the better adsorbent. Further experiments were conducted under different conditions to investigate the optimum adsorption parameters.

3.3. Effect of contact time

The effects of contact time on adsorption of Cr^{6+} and Cu^{2+} ions were investigated by carrying out adsorption experiments for different time duration, that is, 15, 30, 45, 60 and 90 min. Results are indicated in Figs. 4a–d, which indicates that in case of both adsorbents the adsorption rate linearly increases with increasing the contact time. In case of wPS/C/Bt:1:2:2, the maximum adsorption of Cr and Cu ions attained was 77.56% and 79.80%, in 90 min contact time. Similarly, in case of wPET/C/Bt:1:2:2, the maximum adsorption of 90.10% and 86.3% was achieved at a contact

Table 2
Surface properties of the fillers and composite adsorbents

Adsorbent	BJH surface area ($m^2 g^{-1}$)	BET surface area ($m^2 g^{-1}$)	Pore radius (A^0)	Pore volume ($cm^3 g^{-1}$)
Biochar	14.10	18.37	14.90	0.01
Bentonite clay	22.37	43.27	16.62	0.02
wPS/C/Bt:1:2:2	55.59	44.95	27.71	0.07
wPET/C/Bt:1:2:2	50.68	58.53	27.68	0.06

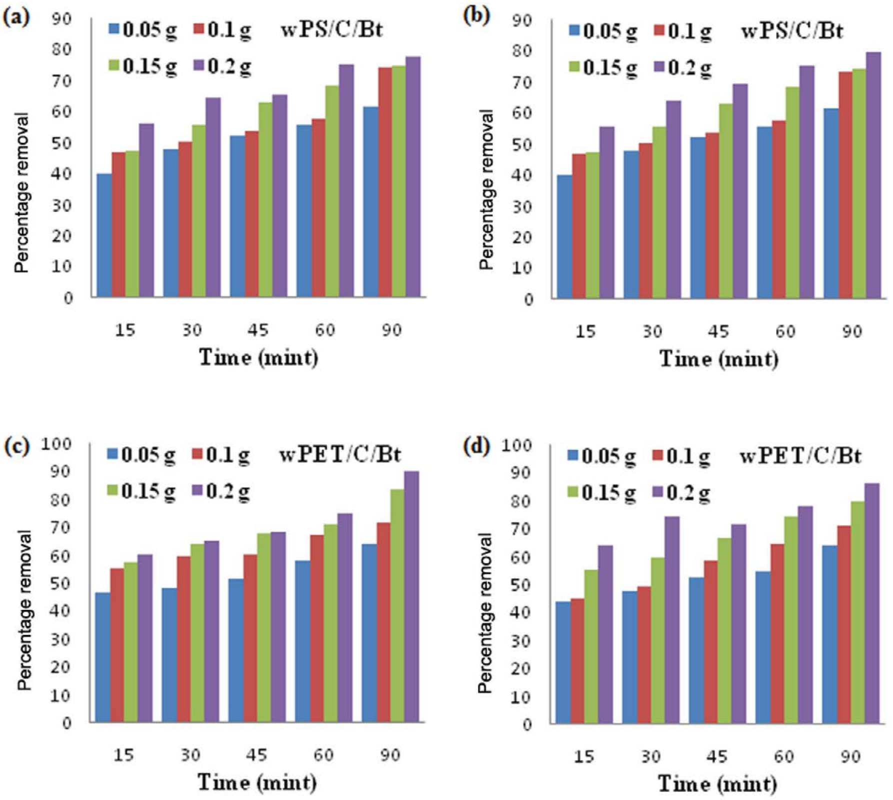

Fig. 4. Effect of contact time on the % adsorption of Cr^{6+} (a, c) and Cu^{2+} (b, d) over the wPS/C/Bt:1:2:2 and wPET/C/Bt:1:2:2 composite.

time of 90 min for Cr and Cu ions, respectively. The experimental data indicate that, the adsorption efficiency of the composites increased by increasing contact time. This is probably due to the higher contact between the surface of the composites and Cr and Cu ions [54]. The system reached equilibrium state after 90 min. Figs. 4a–d also explained that as the initial concentration of solution increased the adsorption efficiency of Cr and Cu ions onto the surface of the adsorbents increased. As clear from the data, the maximum percentage adsorption of Cr and Cu ions was attained for an adsorbent dose of 0.20 g, and after this stage the adsorption became almost constant. The increase in percentage removal of metal ions with increasing adsorbent doses could be attributed to large availability of adsorbent surface area as well as adsorption sites. From that point forward, with additional increment of adsorbent measurement, no critical adsorption effectiveness was noted and this could be a direct result of the congestion of adsorbent particles, which causes covering of adsorption sites [55]. Similar behaviour has been observed in previous studies and arises from the effect of interactions between metal ions and adsorbent. The increased dose is consistent with the greater area and larger number of adsorption sites [56].

3.4. *Effect of temperature*

Figs. 5a–d show the effect of different temperature (30°C, 40°C, 50°C and 60°C) on Cr^{6+} and Cu^{2+} ions over composite adsorbents. Results indicated that as the temperature is increased the adsorption efficiency increases. It is just like as the temperature increases the rate of the reaction also increases. The surface becomes activated and adsorption efficiency increases. In this case, as the temperature increases, the favourable intermolecular forces between adsorbate and adsorbent are much stronger than those between adsorbate and solvent. As a result, the temperature increasing causes adsorbate to be more easily adsorbed. The maximum % adsorption efficiency of wPS/C/Bt:1:2:2 composite was 51.70, 64.62, 67.34 and 76.00 mg g^{-1} for 0.05, 0.10, 0.15 and 0.20 g, respectively, for Cr^{6+}. While in case of Cu^{2+}, this adsorption was 54.68, 58.80, 67.47 and 74.15 mg g^{-1} for 0.05, 0.10, 0.15 and 0.20 g of wPS/C/Bt:1:2:2 composite, respectively. Similarly, the maximum % adsorption efficiency of wPET/C/Bt:1:2:2 composite for Cr^{6+} was 51.36, 60.64, 62.92 and 77.10 mg g^{-1} for 0.05, 0.10, 0.15 and 0.20 g of wPET/C/Bt:1:2:2 composite, respectively. While in case of Cu^{2+}, this adsorption was found to be 55.02, 64.17, 66.99 and 84.10 mg g^{-1} for 0.05, 0.10, 0.15 and 0.20 g of wPET/C/Bt:1:2:2 composite, respectively. The extent of adsorption for both metals increases along with an increase of temperature. In fact, when the temperature increased from 30°C to 60°C, an increase of adsorption was indicating the adsorption process to be endothermic. As temperature increases, the metal ions acquire more energy to overcome the energy barrier between the metals and composites, simultaneously creating more additional adsorption sites on the adsorbent surface due to dissociation of some of the surface components on composites [57]. Moreover, the increasing temperature shows an increased probability of adsorption at higher temperatures, which is consistent with an earlier report [58].

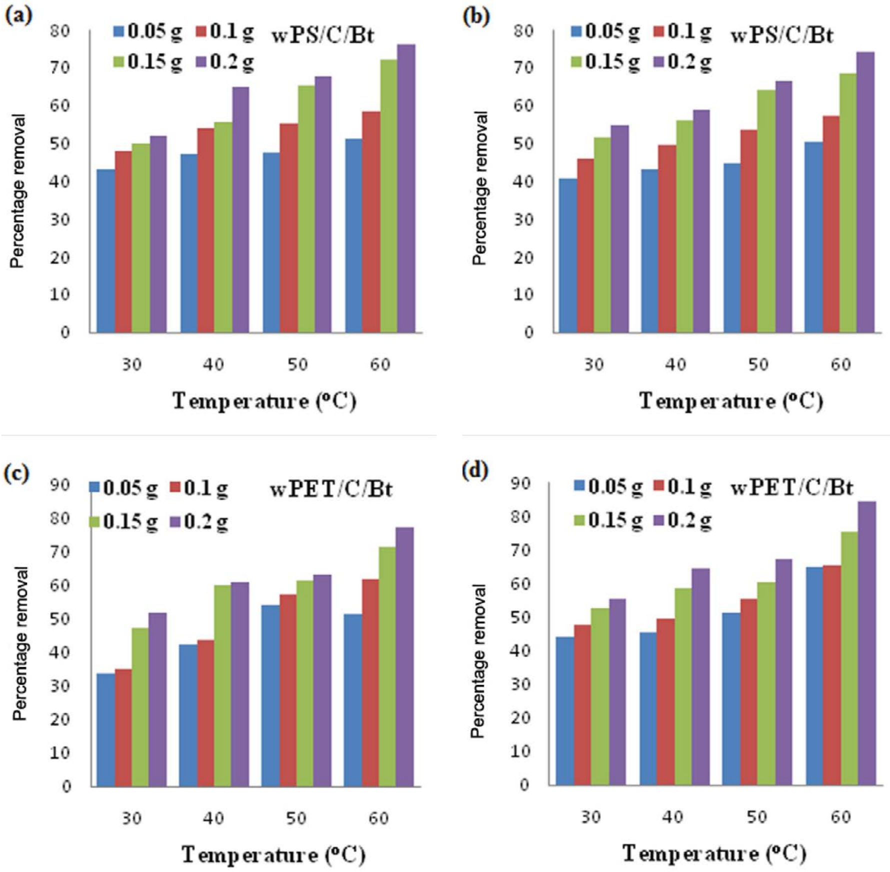

Fig. 5. Effect of temperature on the % adsorption efficiency of the wPS/C/Bt:1:2:2 and wPET/C/Bt:1:2:2 composite on the Cr^{6+} (a, c) and Cu^{2+} (b, d) adsorption.

3.5. Effect of initial concentration of metal ions

Initial concentration of metal ions affects the adsorption and adsorption mechanisms [59]. Generally, adsorption occurs at specific sites when the concentration is low, which are saturated as the concentration increase until it gradually reaches the point where exchange of occupied sites is the only process occurring [59]. Adsorption efficiency of metal was found to increase with the increase in initial concentration of metal ions (Figs. 6a–d). In case of wPS/C/Bt:1:2:2 composite, the adsorptive efficiency of Cr^{6+} increased from 62.58 mg g^{-1} for 10 mg/L to 76.53 mg g^{-1} for 30 mg/L, whereas in case of wPET/C/Bt:1:2:2 composite, the adsorptive efficiency of Cr^{6+} increased from 61.74 mg g^{-1} for 10 mg/L to 97.65 mg g^{-1} for 30 mg/L of initial Cr^{6+} concentration. Similarly, in case of wPS/C/Bt:1:2:2 composite, the adsorptive efficiency of Cu^{2+} was found to be increased from 71.82 to 90.09 mg g^{-1} for an increase in concentration from 10 to 30 mg/L as shown in Figs. 6b and d. While in case of wPET/C/Bt:1:2:2 composite, the adsorption of Cu^{2+} increases to 106.60 mg g^{-1} from 73.60 mg g^{-1} with an increasing of initial metals concentration from 10 to 30 mg/L. This may be due to increasing of initial metals concentration leads to excess availability of metal ions to adsorb over the wPS/C/Bt:1:2:2 and wPET/C/Bt:1:2:2 composites surface active sites. Increasing the initial metal ion concentration led to an increase in adsorption efficiency under different contact times. It may be suggested that the initial concentration provides an important driving force to overcome all mass transfer resistances of metal ions between the aqueous and solid phases, hence a higher initial concentration of metal ions will enhance the adsorption process [60].

3.6. Effect of pH

The pH is an essential parameter of adsorption which primarily influences the interaction of the adsorbent and the state of adsorbate. The effect of pH of the medium on the adsorption of Cr^{6+} and Cu^{2+}ions over the wPS/C/Bt:1:2:2 and wPET/C/Bt:1:2:2 composites was studied under different pH ranging from 1 to 7 (Figs. 7a–d). As above pH 7, most of the metals exist as metal hydroxide which may precipitate in the solution therefore the effect of pH was studied in the neutral and acidic environment. The maximum % adsorption efficiency noted down for Cr^{6+} using 0.05, 0.10, 0.15 and 0.20 g of wPS/C/Bt:1:2:2 composite at pH 3 was 49.65, 55.44, 65.31 and 75.17, respectively. Similarly, the maximum % adsorption efficiency noted down for Cr^{6+} using 0.05, 0.10, 0.15 and 0.20 g of wPET/C/Bt:1:2:2 composite at 3 pH was 51.70, 64.62, 67.34 and 69.31, respectively.

In case of Cr^{6+}, the % adsorption efficiency increases first from pH 1 to 3, and then decreases from pH 4 to 7. Cr is usually found in three ionic forms (i.e., $Cr_2O_7^{2-}$, CrO_4^{2-} and $HCrO_4^-$), and their stability is effected by pH. Cr is found at lower pH

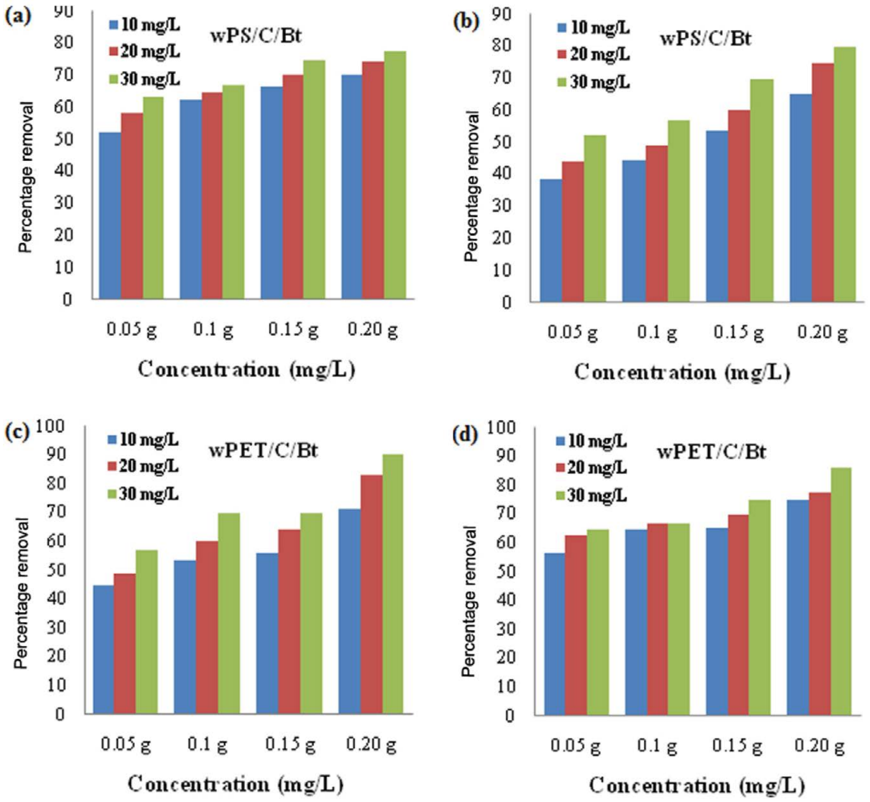

Fig. 6. Effect of initial concentration on the % adsorption efficiency of the wPS/C/Bt:1:2:2 and wPET/C/Bt:1:2:2 composite on the Cr^{6+} (a, c) and Cu^{2+} (b, d) adsorption.

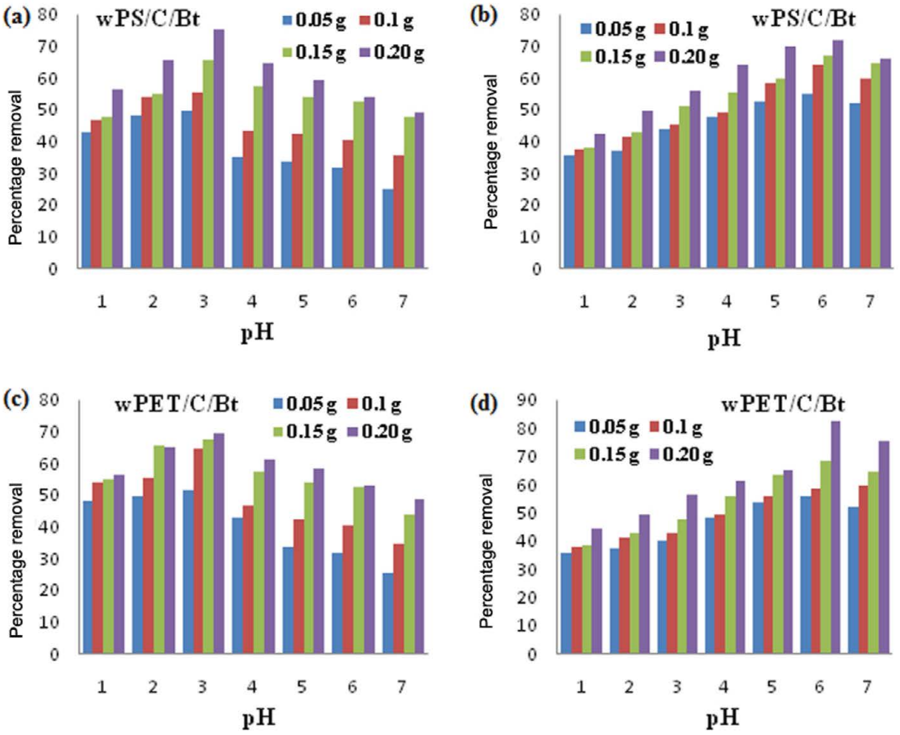

Fig. 7. Effect of pH on the % adsorption efficiency of the wPS/C/Bt:1:2:2 and wPET/C/Bt:1:2:2 composite on the Cr^{6+} (a, c) and Cu^{2+} (b, d) adsorption.

in its HCrO$_4^-$ form, which binds up to the protonated surface of adsorbent due to electrostatic attraction between the negative chromate ions and the positively charged adsorbent surface [61]. It has been shown that pH has profound influence on different forms of Cr ion, for example, Cr$_2$O$_7^{2-}$, CrO$_4^{2-}$ and HCrO$_4^-$ ions [23]. In a solution with pH ranging between 1 and 3, the predominant form of Cr is HCrO$_4^-$ [62], whereas at high pH, HCrO$_4^-$ changes into Cr$_2$O$_7^{2-}$ and CrO$_4^{2-}$ forms, having lower free energy of adsorption, that is, –2.1 to –0.3 kcal/mol.CrO$_4^{2-}$ and Cr$_2$O$_7^{2-}$ are not readily adsorbed, as compared with HCrO$_4^-$ ions wherein the free energy of binding is high, that is, around –2.5 to –0.6 kcal/mol [34]. Hence at low pH the Cr exists in Cr^{3+}, therefore its adsorption rate is high at pH 3.

As shown in Figs. 7b and d, the adsorption of Cu increases gradually as pH increases from 1 to 5, becomes maximum at pH 6, and beyond the adsorption slightly decreases in case of both adsorbents. As indicated by the results at pH of 6, the maximum % adsorption of Cu^{2+} was 55.02, 64.17, 66.99 and 71.66 for 0.05, 0.10, 0.15 and 0.20 g of wPS/C/Bt:1:2:2 composite, respectively. Whereas in case of wPET/C/Bt:1:2:2 composite maximum % adsorption of Cu^{2+} at pH 6 was 55.91, 58.80, 68.56 and 82.22 for 0.05, 0.10, 0.15 and 0.20 g of adsorbent, respectively. The % adsorption efficiency of wPS/C/Bt:1:2:2 and wPET/C/Bt:1:2:2 composites for Cu^{2+} is small at low pH, which might be due to the competition of H$^+$ and Cu^{2+} ions in the solution for the anionic sites on the adsorbent surface. At higher pH, the concentration of H$^+$ decreases, which facilitates the adsorption of Cu cations on the active sites of the adsorbent [63].

In the present experiment, the adsorption of Cu^{2+} was very low when the pH value was less than 5. The adsorption of Cu^{2+} was increased significantly when pH was 6, possibly as a result of the decrease in H$^+$ concentration.

3.7. Kinetic study

The adsorption kinetics of Cr^{6+} and Cu^{2+} ions over wPS/C/Bt:1:2:2 and wPET/C/Bt:1:2:2 composites was studied by applying pseudo-first-order and pseudo-second-order kinetic models (Figs. 8a–d). The pseudo-second order kinetics equation provided a better fit to the adsorption data as compared with pseudo-first-order. Linear plots were obtained with pseudo-second-order kinetics equation, kinetic parameters are indicated in Table 3. The plot of the linearized form of pseudo-second-order model (t/q_t vs. t) is given in Figs. 8a–d.

A good correlation ($R^2 > 0.998$) can be observed, implying that the adsorption occurs via a chemisorption process [64,65]. The experimental data showed the best fit with the highest correlation coefficients ($R^2 \geq 0.998$) for the pseudo-second-order model for both the metal ions. In addition, the experimental values were well matched with the calculated data (Table 3). Therefore, the experimental data accurately support the pseudo-second-order kinetic model for the adsorption of metal ions. This finding indicates that the rate-limiting step was not the resistance of the boundary layer [66]. Thus, the rate-limiting step is chemisorption involving valence forces through the exchange of electrons

Table 3
Pseudo-second-order kinetic parameters for adsorption of Cr^{6+} and Cu^{2+}over composite adsorbents

	wPS/C/Bt:1:2:2		wPET/C/Bt:1:2:2	
	Cr^{6+}	Cu^{2+}	Cr^{6+}	Cu^{2+}
k_2 (mg g^{-1} min^{-1})	0.076	0.075	0.126	0.097
q_{e2} (mg g^{-1})	1.010	1.050	1.216	1.136
R^2	0.999	0.998	0.999	0.999

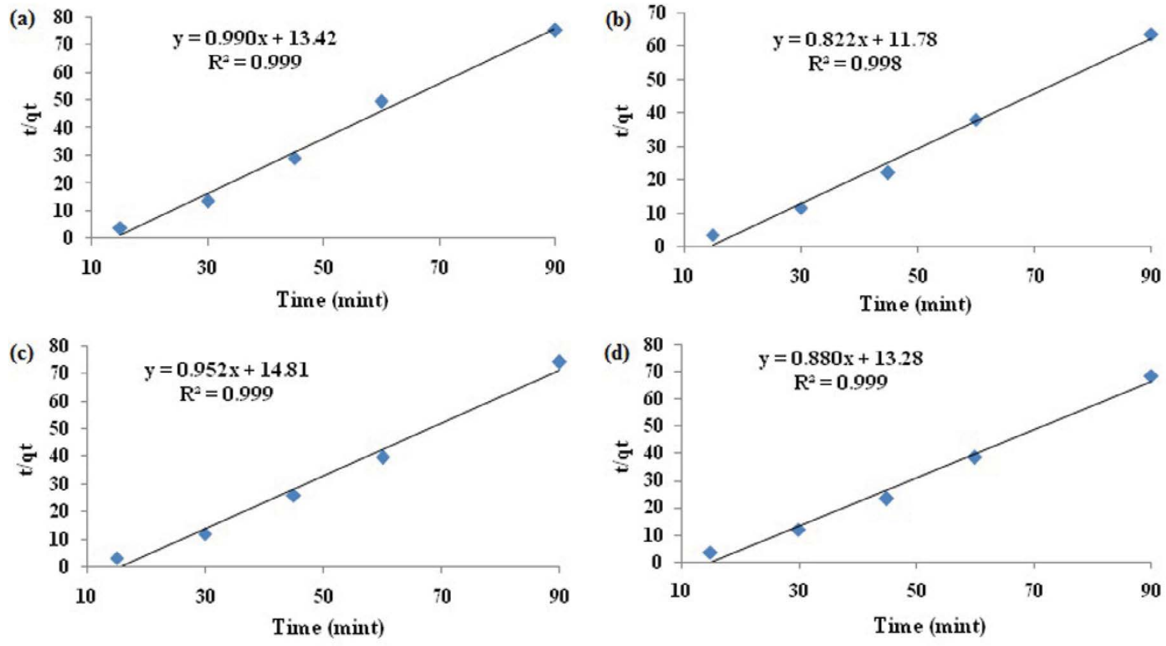

Fig. 8. Pseudo-second-order kinetics for the adsorption of Cr^{6+} (a, b) and Cu^{2+} (c, d) onto wPS/C/Bt:1:2:2 and wPET/C/Bt:1:2:2 composite.

Table 4
Isotherm model parameters for Cr^{6+} and Cu^{2+}adsorption

Langmuir isotherm parameters			Freundlich isotherm parameters		
	wPS/C/Bt:1:2:2			wPS/C/Bt:1:2:2	
	Cr^{6+}	Cu^{2+}		Cr^{6+}	Cu^{2+}
q_m (mg/g)	55.556	55.556	N	1.832	1.953
K_1	0.038	0.035	K_f	2.934	2.881
R^2	0.990	0.981	R^2	0.981	0.996
	wPET/C/Bt:1:2:2			wPET/C/Bt:1:2:2	
	Cr^{6+}	Cu^{2+}		Cr^{6+}	Cu^{2+}
q_m (mg/g)	66.667	7.692	N	3.077	3.356
K_1	0.014	0.008	K_f	2.665	2.639
R^2	0.973	0.994	R^2	0.924	0.999

between the metal ions and the different functional groups in the adsorbent [67]. For the two composites, the adsorption isotherm equations of Cr^{6+} and Cu^{+2} were a better fit with the Lagergren second-order equation, indicating that the adsorption process followed Lagergren second-order mechanism and adsorption rate was controlled by chemical adsorption [68], and the particle dispersion mechanism played a dominant role in the whole adsorption process. Several authors have also reported the applicability of the pseudo-second-order kinetic model for modelling the removal of copper using other sorbents [69,70].

3.8. Isotherm study

The equilibrium adsorption data were evaluated using the Freundlich and Langmuir isotherm models. The calculated Langmuir constants (K_1 and q_m) and Freundlich constants (n and K_f) as well as the coefficients of correlation (R^2) for both isotherms are given in Table 4.

Figs. 9a and b show the plots of Langmuir for adsorption of Cr^{6+} and Figs. 10a and b show Freundlich isotherms for Cu^{2+} over wPS/C/Bt:1:2:2 and wPET/C/Bt:1:2:2 composites. The straight line plots of Freundlich and Langmuir isotherm models demonstrate that the Cr^{6+} adsorption on wPS/C/Bt:1:2:2 and wPET/C/Bt:1:2:2 composites follows Langmuir isotherm; whereas the Cu^{2+} adsorption on wPS/C/Bt:1:2:2 and wPET/C/Bt:1:2:2 composite follows Freundlich isotherm. The results suggest that in case of Cr^{6+} the Langmuir model best fits the data as shown by the correlation coefficient >0.990 and 0.973, whereas in case of Cu^{2+} the Freundlich model best fits the data as shown by the correlation coefficient >0.996 and 0.999. This result demonstrates that adsorption on a heterogeneous surface. It also assumes that the adsorption efficiency of the adsorbent increases with increasing concentration of the adsorbate, which is in agreement with the results obtained for the effect of initial concentration on adsorption.

3.9. Thermodynamic studies

The feasibility, thermal effect and spontaneity of the adsorption process were calculated from the variation of the thermodynamic equilibrium constant, K_D, with temperature.

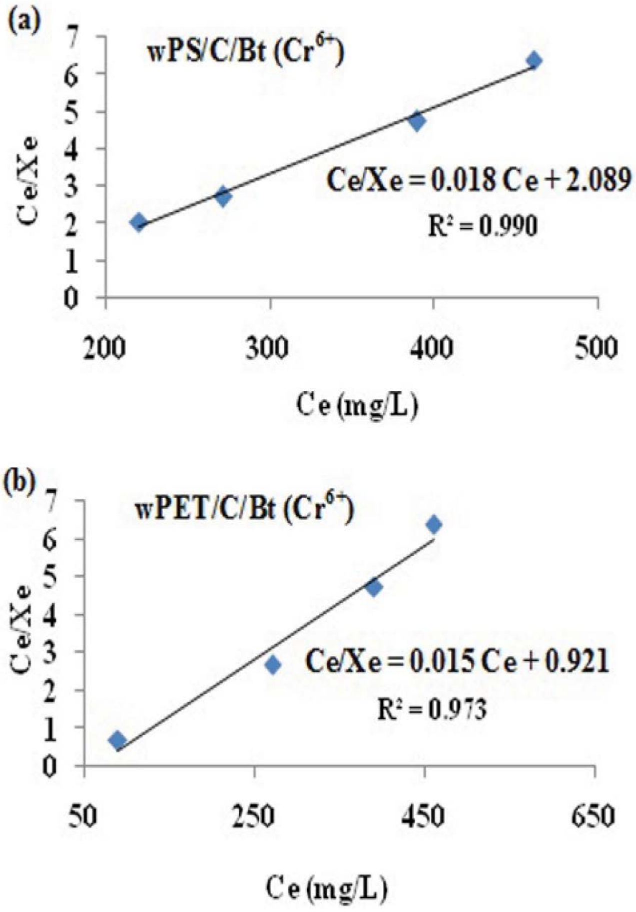

Fig. 9. Langmuir isotherms for Cr^{6+} adsorption over wPS/C/Bt:1:2:2 (a) and wPET/C/Bt:1:2:2 (b) composites.

Thermodynamic parameters such as the free energy change ($\Delta G°$), enthalpy change ($\Delta H°$) and entropy change ($\Delta S°$) were calculated using the following equations [71,72]:

$$\Delta G° = -RT \ln K_D \quad (7)$$

Table 5
Thermodynamic parameters for the adsorption of Cr^{6+} and Cu^{2+} onto wPS/C/Bt:1:2:2 and wPET/C/Bt:1:2:2

wPS/C/Bt:1:2:2						
Temperature (°C)	Cr^{6+}			Cu^{2+}		
	ΔG° (kJ mol^{-1})	ΔH° (kJ mol^{-1})	ΔS° (kJ mol^{-1})	ΔG° (kJ mol^{-1})	ΔH° (kJ mol^{-1})	ΔS° (kJ mol^{-1})
30	–4.6763	9.6526	0.0329	–4.8693	8.4470	0.0289
40	–4.0430			–4.2384		
50	–2.6785			–3.0255		
60	–1.9799			–1.4481		
wPET/C/Bt:1:2:2						
30	–4.2830	10.010	0.0342	–3.2281	2.8592	0.0093
40	–3.6734			–3.1760		
50	–2.7668			–2.1098		
60	–1.8201			–0.1443		

Table 6
Comparison of different adsorbents used for Cr and Cu ions removal

	Adsorption potential		
Adsorbent	Cr^{6+}	Cu^{2+}	References
Polyaniline/palygorskite composite, mg g^{-1}	198	114	[34]
Polyaniline, mg g^{-1}	101	92	[34]
Activated carbon, mg g^{-1}	34.70	24.21	[35]
Expanded perlite, mg g^{-1}	–	8.62	[36]
Acid-activated palygorskite, mg g^{-1}	–	32.24	[37]
Crosslink cationic starch, mg g^{-1}	97.08	–	[38]
Palygorskite, mg g^{-1}	30.70	–	[18]
wPS/C/Bt:1:2:2, mg g^{-1}	107.88	109.65	This article
wPET/C/Bt:1:2:2, mg g^{-1}	127	118.65	This article

$$\Delta H^\circ = R\frac{T_2 T_1}{T_2 - T_1}\ln\frac{k_2}{k_1} \tag{8}$$

$$\Delta S^\circ = \frac{\Delta H^\circ - \Delta G^\circ}{T} \tag{9}$$

The negative values of ΔG° in Table 5 show the spontaneous and feasibility nature of Cr^{6+} and Cu^{2+} adsorption onto wPS/C/Bt:1:2:2 and wPET/C/Bt:1:2:2. As the temperature is increased, the value of ΔG° increases, indicating that at higher temperature the degree of spontaneity also increased. The positive value of ΔH° and ΔS° confirms the endothermic nature of the adsorption process.

3.10. Comparison of adsorption potential of different adsorbents

The comparative adsorption efficiency of the various adsorbents reported in literature and the composite adsorbents, that is, wPS/C/Bt:1:2:2 and wPET/C/Bt:1:2:2 for Cr and Cu ions adsorption is summarized in Table 6. It is clear from the data that the adsorption efficiency of the wPET/C/Bt:1:2:2 composite is superior to that of wPS/C/Bt:1:2:2 adsorbents. In addition, by comparing the adsorption efficiency for Cr^{6+} and Cu^{2+} displayed in Table 6, the adsorption of metal ions from the single-metal solutions was in the order: $Cr^{6+} > Cu^{2+}$, and the adsorption efficiency for Cr^{6+} was much larger than Cu^{2+}. The difference for adsorption efficiency of Cr^{6+} and Cu^{2+} could be attributed to the fact that Cr^{6+} is not a hexavalent chromium cation but occurs as chromate/dichromate anion interacting with the adsorbent, which is quite different from other metal cations.

4. Conclusions

The wPS/C/Bt:1:2:2 and wPET/C/Bt:1:2:2 composites were synthesized by a simple and low-cost method. The wPET/C/Bt:1:2:2 composite formed is an effective adsorbent for toxic metals such as Cr^{6+} and Cu^{2+} removal from aqueous medium. SEM, FTIR and SAA were employed to characterize its surface morphology, functional groups and average pore radius, total pore volume and specific surface area. The synthesized composites were used as an adsorbent to remove Cr and Cu ions from an aqueous solution. The removal of metal ions was greatly dependent on adsorption parameters, including pH, contact time, temperature, adsorbent dose and initial concentration. The results showed that the adsorption kinetics followed pseudo-second-order kinetics. The study

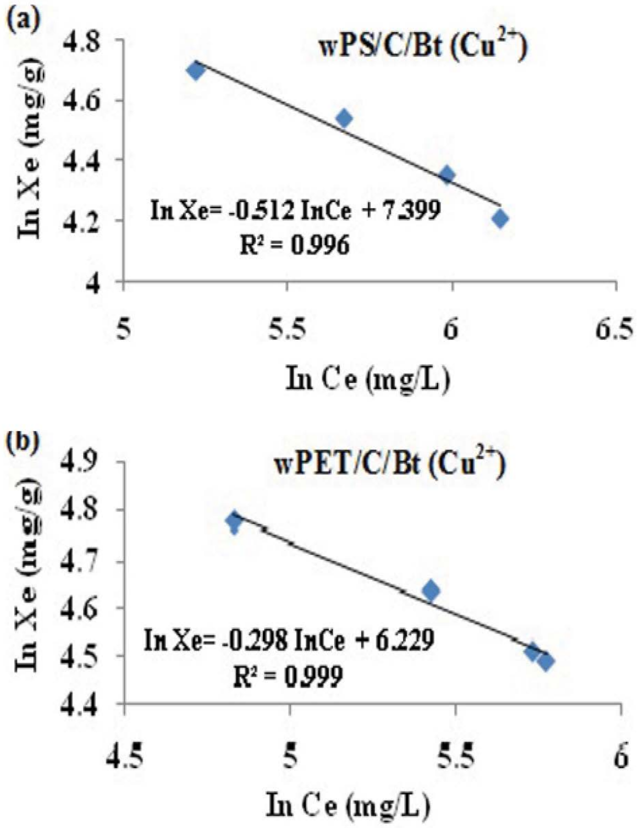

Fig. 10. Freundlich isotherms for Cu^{2+} adsorption over wPS/C/Bt:1:2:2 (a) and wPET/C/Bt:1:2:2 (b) composites.

revealed that Freundlich equation represented the best fit of experimental data for Cr^{6+}, whereas the Cu^{2+} adsorption on wPET/C/Bt:1:2:2 composite follows Langmuir isotherm. Thermodynamic results which indicate that adsorption of Cr^{6+} and Cu^{2+} onto wPS/C/Bt:1:2:2 and wPET/C/Bt:1:2:2 is endothermic in nature. The maximum percentage adsorption efficiency of Cr^{6+} and Cu^{2+} from aqueous medium was 90.10 and 86.30, respectively. These results indicate that the wPET/C/Bt:1:2:2 can be used as a suitable and efficient adsorbent in the removal of Cr^{6+} and Cu^{2+} from wastewater. This study not only helps to remove toxic Cr^{6+} and Cu^{2+} from wastewater, but also serves to provide a route for better reuse of the waste plastic materials thereby minimizing the environmental degradation due to waste plastic.

Acknowledgement

The authors are very thankful to the staffs of the Centralized Resource Laboratories and Materials Research Laboratory, University of Peshawar for providing instrumental facility.

References

[1] M. Ilyas, W. Ahmad, H. Khan, S. Yousaf, M. Yasir, A. Khan, Environmental and health impacts of industrial wastewater effluents in Pakistan: a review, Rev. Environ. Health, 34 (2019) 171–186.

[2] K.A. Kaushik, S.J. Dalal, S. Panwar, Impact of industrialization on culture of Uttarakhand and its role on career enhancement, VSRD Int. J. Bus Manage. Res., 2 (2012) 123–132.

[3] EPA. Constructed wetlands for wastewater treatment and wildlife habitat, (1993). Available from http://www.epa.gov/owow/wetlands/construct.

[4] M. McCasland, N.M. Trautmann, R.J. Wagenet, Nitrate: Health effects in drinking water, (1985). Available from http://pmep.cee.comell.edu/facts.slides–self/facts/nit-heefgrw85.

[5] E.A. El-Sharkawy, Adsorption of textile dyes on to activated carbons synthesized from solid waste: decolourizing power in relation to surface properties, Adsorpt. Sci. Technol., 19 (2001) 795–811.

[6] S. Chaudhari, V. Tare, Removal and recovery of heavy metals from simulated wastewater using insoluble starch Xanthate process, Pract. Period Hazard Toxic. Radioact. Waste Manage., 12 (2008) 170–180.

[7] B.M. Braukman, Industrial solutions amenable to biosorption, in: B. Volesky (Ed.), Biosorption of Heavy Metals, CRC Press, USA. (1990) pp. 51–64.

[8] K. Shekhawat, S. Chatterjee, B. Joshi, Chromium toxicity and its health hazards, Int. J. Adv. Res., 3 (2015) 167–172.

[9] J.W. Ball, J.A. Izbicki, Occurrence of hexavalent chromium in ground water in the western Mojave Desert, California, Appl. Geochem., 19 (2004) 1123–1135.

[10] D. Fantoni, G. Brozzo, M. Canepa, F. Cipolli, L. Marini, G. Ottonello, M. Zuccolini, Natural hexavalent chromium in groundwaters interacting with ophiolitic rocks, Environ. Geol., 42 (2002) 871–882.

[11] F.N. Azad, M. Ghaedi, K. Dashtian, A. Jamshidi, G. Hassani, M. Montazerozohori, S. Hajati, M. Rajabi, A.A. Bazrafshan, Preparation and characterization of an AC–Fe_3O_4–Au hybrid for the simultaneous removal of Cd^{2+}, Pb^{2+}, Cr^{3+} and Ni^{2+} ions from aqueous solution via complexation with 2-((2, 4-dichlorobenzylidene)-amino)-benzenethiol: Taguchi optimization, RSC Adv., 6 (2016) 19780–19791.

[12] L.S. Thakur, M. Parmar, Adsorption of heavy metal (Cu^{2+}, Ni^{2+} and Zn^{2+}) from synthetic waste water by tea waste adsorbent, Int. J. Chem. Phys. Sci., 2 (2013) 6–19.

[13] P. Parker, Encyclopaedia of Environmental Science, 2nd ed., Mc- Graw Hill, NewYork, 1980.

[14] M. Sitting, Toxic Metals—Pollution Control and Worker Protection, Noyes Data Corporation, New Jersey, 1976.

[15] K. Kadirvelu, Preparation and characterization of activated carbon, from coir pith and its application to metal bearing wastewater, Ph.D. Thesis, Bharathiar University, Coimbatore, India, 1998.

[16] S. Yang, X. Ren, G. Zhao, W. Shi, G. Montavon, B. Grambow, X. Wang, Competitive sorption and selective sequence of Cu (II) and Ni (II) on montmorillonite: batch, modeling, EPR and XAS studies, Geochim. Cosmochim. Acta, 166 (2015) 129–145.

[17] E. Eren, Removal of copper ions by modified Unye clay, Turkey, J. Hazard. Mater., 159 (2008) 235–244.

[18] J.H. Potgieter, S.S. Potgieter-Vermaak, P.D. Kalibantonga, Heavy metals removal from solution by palygorskite clay, Miner Eng., 19 (2006) 463–470.

[19] R. Camarillo, Á. Pérez, P. Cañizares, A. de Lucas, Removal of heavy metal ions by polymer enhanced ultrafiltration: batch process modeling and thermodynamics of complexation reactions, Desalination, 286 (2012) 193–199.

[20] R. Aravindhan, B. Madhan, J.R. Rao, B.U. Nair, T. Ramasami, Bioaccumulation of chromium from tannery wastewater: an approach for chrome recovery and reuse, Environ. Sci. Technol., 38 (2004) 300–306.

[21] J.J. Testa, M.A. Grela, M.I. Litter, Heterogeneous photocatalytic reduction of chromium (VI) over TiO_2 particles in the presence of oxalate: involvement of Cr (V) species, Environ. Sci. Technol., 38 (2004) 1589–1594.

[22] C.A. Kozlowski, W. Walkowiak, Removal of chromium (VI) from aqueous solutions by polymer inclusion membranes, Water Res., 36 (2002) 4870–4876.

[23] V.K. Gupta, A.K. Shrivastava, N. Jain, Biosorption of chromium (VI) from aqueous solutions by green algae Spirogyra species, Water Res., 35 (2001) 4079–4085.

[24] H.F. Shaalan, M.H. Sorour, S.R. Tewfik, Simulation and optimization of a membrane system for chromium recovery from tanning wastes, Desalination, 141 (2001) 315–324.

[25] J.C. Seaman, P.M. Bertsch, L. Schwallie, In situ Cr (VI) reduction within coarse-textured, oxide-coated soil and aquifer systems using Fe (II) solutions, Environ. Sci. Technol., 33 (1999) 938–944.

[26] S.K. Srivastava, V.K. Gupta, D. Mohan, Removal of lead and chromium by activated slag—a blast-furnace waste, J. Environ. Eng., 123 (1997) 461–468.

[27] D. Petruzzelli, R. Passino, G. Tiravanti, Ion exchange process for chromium removal and recovery from tannery wastes, Ind. Eng. Chem. Res., 34 (1995) 2612–2617.

[28] S. Schiewer, S.B. Patil, Modeling the effect of pH on biosorption of heavy metals by citrus peels, J. Hazard. Mater., 157 (2008) 8–17.

[29] J. Wu, Y. Wei, J. Lin, S. Lin, Study on starch-graft-acrylamide/mineral powder superabsorbent composite, Polymer, 44 (2003) 6513–6520.

[30] W.F. Lee, Y.C. Chen, Effect of intercalated reactive mica on water absorbency for poly (sodium acrylate) composite superabsorbents, Eur. Polym. J., 41 (2005) 1605–1612.

[31] K. Ibrahim, H. Khoury, Use of natural chabazite–phillipsite tuff in wastewater treatment from electroplating factories in Jordan, Environ. Geol., 41 (2002) 547–551.

[32] L. Monser, N. Adhoum, Modified activated carbon for the removal of copper, zinc, chromium and cyanide from wastewater, Sep. Purif. Technol., 26 (2002) 137–146.

[33] V. Sarin, K. Pant, Removal of chromium from industrial waste by using eucalyptus bark, Bioresour. Technol., 97 (2006) 15–20.

[34] Y. Kong, J. Wei, Z. Wang, T. Sun, C. Yao, Z. Chen, Heavy metals removal from solution by polyaniline/palygorskite composite, J. Appl. Polym. Sci., 122 (2011) 2054–2059.

[35] M. Kobya, E. Demirbas, E. Senturk, M. Ince, Adsorption of heavy metal ions from aqueous solutions by activated carbon prepared from apricot stone, Bioresour. Technol., 96 (2005) 1518–1521.

[36] A. Sarı, M. Tuzen, D. Cıtak, M. Soylak, Adsorption characteristics of Cu (II) and Pb (II) onto expanded perlite from aqueous solution, J. Hazard. Mater., 148 (2007) 387–394.

[37] H. Chen, Y. Zhao, A. Wang, Removal of Cu (II) from aqueous solution by adsorption onto acid-activated palygorskite, J. Hazard. Mater., 149 (2007) 346–354.

[38] S.M. Xu, J. Wei, S. Feng, J.D. Wang, X.S. Li, A study in the adsorption behaviors of Cr (VI) on crosslinked cationic starches, J. Polym. Res., 11 (2004) 211–215.

[39] R.S. Chauhan, S. Gopinath, P. Razdan, C. Delattre, G.S. Nirmala, R. Natarajan, Thermal decomposition of expanded polystyrene in a pebble bed reactor to get higher liquid fraction yield at low temperatures, Waste Manage., 28 (2008) 2140–2145.

[40] K. Saido, K. Amamiya, H. Sato, A. Okabe, N. Ogawa, Y. Kamaya, T. Kusui, Analysis of styrene oligomer contaminants generated from marine debris polystyrene on the coast of Okinawa, Bunseki Kagaku/Japan Analyst, 61 (2012).

[41] M. Ilyas, W. Ahmad, H. Khan, S. Yousaf, K. Khan, S. Nazir, Plastic waste as a significant threat to environment–a systematic literature review, Rev. Environ. Health, 33 (2018) 383–406.

[42] R. Donat, A. Akdogan, E. Erdem, H. Cetisli, Thermodynamics of Pb^{2+} and Ni^{2+} adsorption onto natural bentonite from aqueous solutions, J. Colloid Interface Sci., 286 (2005) 43–52.

[43] Y.S. Ho, G. McKay, Sorption of dye from aqueous solution by peat, Chem. Eng. J., 70 (1998) 115–124.

[44] S. Chen, J. Zhang, C. Zhang, Q. Yue, Y. Li, C. Li, Equilibrium and kinetic studies of methyl orange and methyl violet adsorption on activated carbon derived from *Phragmites australis*, Desalination, 252 (2010) 149–156.

[45] M. Lawrinenko, Anion exchange capacity of biochar, Graduate theses, Iowa State University, 2014.

[46] Y. Yao, B. Gao, J. Fang, M. Zhang, H. Chen, Y. Zhou, L. Yang, Characterization and environmental applications of clay–biochar composites, Chem. Eng. J., 242 (2014) 136–143.

[47] M. Edge, R. Wiles, N.S. Allen, W.A. McDonald, S.V. Mortlock, Characterisation of the species responsible for yellowing in melt degraded aromatic polyesters—I: Yellowing of poly (ethylene terephthalate), Polym. Degrad. Stab., 53 (1996) 141–151.

[48] T.M. Piqué, A. Vázquez, Uso de EspectroscopíaInfrarroja con Transformada de Fourier (FTIR) en el estudio de la hidratación del cemento. Concreto y cement, Investigación y desarrollo, 3 (2012) 62–71.

[49] R.M. Silverstein, F.X. Webster, 13C NMR spectrometry. Spectrometric identification of organic compounds, 1998, pp. 217–249.

[50] M.A. Tantawy, M.R. Shatat, A.M. El-Roudi, M.A. Taher, M. Abd-El-Hamed, Low temperature synthesis of belite cement based on silica fume and lime, Int. Sch. Res. Notices, (2014) 1–10, http://dx.doi.org/10.1155/2014/873215.

[51] M. Chollet, M. Horgnies, Analyses of the surfaces of concrete by Raman and FT-IR spectroscopies: comparative study of hardened samples after demoulding and after organic post treatment, Surf. Interface Anal., 43 (2011) 714–725.

[52] V. Herman, H. Takacs, F. Duclairoir, O. Renault, J.H. Tortai, B. Viala, Core double–shell cobalt/graphene/polystyrene magnetic nanocomposites synthesized by in situ sonochemical polymerization, RSC Adv., 5 (2015) 51371–51381.

[53] M. Subramani, U. Sepperumal. FTIR analysis of bacterial mediated chemical changes in Polystyrene foam, Ann. Biol. Res., 7 (2016) 55–61.

[54] D. Suteu, M. Badeanu, T. Malutan, A.I. Chirculescu, Valorization of food wastes (orange seeds) as adsorbent for dye retention from aqueous medium, Desal. Wat. Treat., 57 (2016) 29070–29081.

[55] A. Ahmadpour, M. Tahmasbi, T.R. Bastami, J.A. Besharati, Rapid removal of cobalt ion from aqueous solutions by almond green hull, J. Hazard. Mater., 30 (2009) 925–930.

[56] H. Liu, S. Liang, J. Gao, H.H. Ngo, W. Guo, Z. Guo, J. Wang, Y. Li, Enhancement of Cr (VI) removal by modifying activated carbon developed from *Zizania caduciflora* with tartaric acid during phosphoric acid activation, Chem. Eng. J., 246 (2014) 168–174.

[57] S. Athapaththu, "A comprehensive study of Cd (II) removal from aqueous solution via adsorption and solar photocatalysis," Electronic Thesis and Dissertation Repository, vol. 19 (2013) p. 1783.

[58] K.G. Bhattacharyya, S.S Gupta, Pb (II) uptake by kaolinite and montmorillonite in aqueous medium: influence of acid activation of the clays, Colloids Surf. A Physicochem. Eng. Asp., 277 (2006) 191–200.

[59] C.L. Massocatto, E.C. Paschoal, N. Buzinaro, T.F. Oliveria, C.R.T. Tarley, J. Caetano, K.M. Diniz, Preparation and evaluation of kinetics and thermodynamics studies of lead adsorption onto chemically modified banana peels, Desal. Wat. Treat., 51 (2013) 5682–5691.

[60] A. Saeed, M. Iqbal, M.W. Akhtar, Removal and recovery of lead (II) from single and multimetal (Cd, Cu, Ni, Zn) solutions by crop milling waste (black gram husk), J. Hazard. Mater., 117 (2005) 65–73.

[61] Z. Melichová, L. Hromada, Adsorption of Pb^{2+} and Cu^{2+} ions from aqueous solutions on natural bentonite, Pol. J. Environ. Stud., 22 (2013) 457–464.

[62] S.Y. Wang, Y.K. Tang, K. Li, Y.Y. Mo, H.F. Li, Z.Q. Gu, Combined performance of biochar sorption and magnetic separation processes for treatment of chromium-contained electroplating wastewater, Bioresour. Technol., 174 (2014) 67–73.

[63] P. Yuan, M. Fan, D. Yang, H. He, D. Liu, A. Yuan, T. Chen, Montmorillonite-supported magnetite nanoparticles for the removal of hexavalent chromium [Cr (VI)] from aqueous solutions, J. Hazard. Mater., 166 (2009) 821–829.

[64] H. Niu, X.S. Xu, J.H. Wang, B. Volesky, Removal of lead from aqueous solutions by Penicillium biomass, Biotechnol. Bioeng., 42 (1993) 785–787.

[65] W.M. Antunes, A.S. Luna, C.A. Henriques, A.C.A. da Costa, An evaluation of copper biosorption by a brown seaweed under optimized conditions, Electron. J. Biotechnol., 6 (2003) 174–184.

[66] H. Tounsadi, A. Khalidi, M. Abdennouri, N. Barka, Biosorption potential of *Diplotaxis harra* and *Glebionis coronaria* L. biomasses for the removal of Cd (II) and Co (II) from aqueous solutions, J. Environ. Chem. Eng., 3 (2015) 822–830.

[67] M. Rahman, K.V. Sathasivam, Heavy metal adsorption onto *Kappaphycus* sp. from aqueous solutions: the use of error functions for validation of isotherm and kinetics models, Biomed. Res. Int., 2015 (2015) 1–13.

[68] W.M. Ibrahim, Biosorption of heavy metal ions from aqueous solution by red macroalgae, J. Hazard. Mater., 192 (2011) 1827–1835.

[69] K.G. Bhattacharyya, S.S. Gupta, Kaolinite, montmorillonite, and their modified derivatives as adsorbents for removal of Cu (II) from aqueous solution, Sep. Purif. Technol., 50 (2006) 388–397.

[70] M. Hamidpour, M. Kalbasi, M. Afyuni, H. Shariatmadari, G. Furrer, Sorption of lead on Iranian bentonite and zeolite: kinetics and isotherms, Environ. Earth Sci., 62 (2011) 559–568.

[71] W. Konicki, I. Pełech, E. Mijowska, I. Jasińska, Adsorption of anionic dye Direct Red 23 onto magnetic multi-walled carbon nanotubes-Fe_3C nanocomposite: kinetics, equilibrium and thermodynamics, Chem. Eng. J., 210 (2012) 87–95.

[72] V.K. Gupta, C. Jain, I. Ali, M. Sharma, V. Saini, Removal of cadmium and nickel from wastewater using bagasse fly ash—a sugar industry waste, Water Res., 37 (2003) 4038–4044.